Controlling mesenchymal stem cell differentiation using vanadium oxide thin film surface wettability

Mariya Khokhlova, Abhishek Yadav, M. Hammad, Eva Lhuissier, R. Retoux, D. Goux, Arnaud Fouchet, Adrian David, Ulrike Luders, Karim Boumediene, et al.

APL Materials

RESEARCH ARTICLE | JULY 05 2023

Controlling mesenchymal stem cell differentiation using vanadium oxide thin film surface wettability

Maria Khokhlova ; Abhishek Yadav ; M. Hammad; Eva Lhuissier; R. Retoux; D. Goux; Arnaud Fouchet ; Adrian David ; Ulrike Luders ; Karim Boumediene ; W. Prellier

APL Mater 11, 071102 (2023)
https://doi.org/10.1063/5.0155299

Controlling mesenchymal stem cell differentiation using vanadium oxide thin film surface wettability

Cite as: APL Mater. 11, 071102 (2023); doi: 10.1063/5.0155299
Submitted: 19 April 2023 • Accepted: 14 June 2023 •
Published Online: 5 July 2023

Maria Khokhlova,[1,2] Abhishek Yadav,[1] M. Hammad,[2] Eva Lhuissier,[2] R. Retoux,[1] D. Goux,[1,3] Arnaud Fouchet,[1] Adrian David,[1] Ulrike Luders,[1] Karim Boumediene,[2] and W. Prellier[1,a)]

AFFILIATIONS

[1] Laboratoire CRISMAT, CNRS UMR 6508, ENSICAEN, UNICAEN, Normandie Université, 6 Bd Maréchal Juin, F-14050 Caen Cedex 4, France
[2] Normandie Université, UR7451 BIOCONNECT, 14000 Caen, France
[3] ICORE, SF 4206, UNICAEN, Esplanade de la Paix, 14032 Caen Cedex 5, France

[a)] **Author to whom correspondence should be addressed:** wilfrid.prellier@ensicaen.fr

ABSTRACT

Although vanadium compounds are well recognized for their ability to change from insulator to metal, they may also be used therapeutically to address significant medical issues. In this study, we used vanadium oxide thin films synthesized by the pulsed laser deposition (PLD) technique to examine human stem cells generated from bone marrow. According to x-ray reflectivity (XRR) measurements, the films' thickness ranged from 6 to 26 nm. The water contact angle method has been employed to probe the surface energy and wettability of the films, which influence the cell behavior significantly. We also used a variety of techniques, such as differentiation staining, phase contrast microscopy, and real-time reverse transcription-polymerase chain reaction (RT-PCR), to examine the growth, adhesion, proliferation, and differentiation of human bone marrow mesenchymal stem cells (hBMMSCs) on these oxide films over time. Our results indicated that vanadium oxide films alter hBMMSCs adhesion and growth and affect their differentiation. The application of VO_x films in biological and medical materials, as well as future research on cells, is all made possible by these findings, which also improve our understanding of the biological actions of vanadium compounds.

I. INTRODUCTION

Over the last four decades, oxide materials have garnered much interest in the scientific community. For example, high T_C superconductivity and colossal magnetoresistance, discovered during this period, have opened up exciting opportunities for various applications for oxides, including those in electronics, transparent oxides, optoelectronics, magnetoelectronics, thermoelectrics, piezo electronics, energy harvesting, and hydrogen storage.[1–3] Despite the vast range of applications for oxide materials, their potential use in medical and biological fields is relatively unexplored.[4] Titanium oxide (TiO_2), in the form of nanotubes or thin films, has been extensively studied and utilized in biomedical implants because of its bio-inertness and good biocompatibility.[5–7] However, other metal oxides have yet to be explored. Among these, vanadium oxide (VO_x) is a promising candidate for biomedical implants since it occurs on the surface of a commonly used implant material, TiAlV alloy.[6] However, since most metal implants are inert, the release of vanadium ions from the surface of a biomaterial can lead to adverse effects.[7,8] Conversely, some studies have shown that vanadium compounds can effectively enhance cell growth at relatively low concentrations of released vanadium ions (up to 10 μM).[8,9] Therefore, understanding the interfacial interactions between vanadium oxide compounds and living materials is crucial.

Because of their potential for self-renewal and differentiation into a variety of cell types, mesenchymal stem cells have garnered

much interest in the fields of regenerative medicine and tissue engineering.[10] So far, only TiO_2 and Al_2O_3 have been investigated for their potential to modulate cell growth and differentiation depending on their composition.[4] Therefore, more research into alternative oxide surfaces is required. In addition, bio-interface engineering relies heavily on being able to exert command over cellular architecture, particularly in the context of shrunken dimensions.[11] One of the primary goals of tissue engineering is the development of a structural environment conducive to the survival and expansion of progenitor cells.[12,13]

This article aims to prepare the VO_x thin films on glass surfaces using the pulsed laser deposition (PLD) technique and examine the adhesion, proliferation, and differentiation of human bone marrow mesenchymal stem cells (hBMMSCs) on the surfaces of such films in comparison with uncoated glass and plastic cover slides. We found that vanadium oxide films can affect their differentiation. This study offers new insights into using thin oxide films as culture substrates for developing in vitro tests and related medical applications such as articular prostheses.

II. MATERIALS AND METHODS

A. Preparation and characterization of oxide thin films

However, while other techniques such as reactive sputtering, chemical vapor deposition, and molecular beam epitaxy have been used to prepare and generate such films in the past,[14,15] the PLD has proven to be more reproducible and reliable for oxides; thus, vanadium oxide thin films were deposited on the glass substrates using the pulsed laser deposition (PLD) technique.[16] A target of vanadium oxide was prepared by a standard solid-state route, and the films were deposited onto the glass substrates using a KrF excimer laser source (λ = 248 nm). The laser frequency was kept constant at 5 Hz, and the number of pulses was varied to achieve different film thicknesses. For instance, a sample with 5000 pulses resulted in a vanadium oxide thin film with a thickness of 19 nm. The deposition process was carried out at 400 °C, after evacuating the vacuum chamber to a base pressure lower than 1.33×10^{-4} Pa (10^{-6} Torr). The samples were characterized using x-ray reflectivity (XRR) measurements with a Bruker™ D8 Discover diffractometer. The measurements were taken using CuKα_1 radiation (λ = 1.541 Å) over a 2θ angular range from 0° to 6°. The thickness of the films was determined from the slope of the relative position of the oscillation maxima vs the square of their order number. Reflectivity curves were plotted using x-ray diffraction (XRD) measurements over an angular range of 10°–50°.

The topography was characterized using Atomic Force Microscopy (AFM) with the PicoSPM™ technique.[17] Root-mean-square (rms) roughness was determined from AFM measurements of a 1 μm^2 area in the tapping mode and calculated using WSxM 5.0 software. In addition, we investigated the relationship between roughness and wettability by measuring the wettability, as described by Wenzel[18]

$$\cos(\theta_m) = r\cos(\theta_y), \tag{1}$$

where θ_m is the measured contact angle, θ_y is Young's contact angle, and r is the roughness ratio (r = 1 for a smooth surface and >1 for a rough one). The roughness ratio (r) is defined as the ratio of the developed surface area of the film to its nominal area. Wettability is a solid–liquid–vapor interfacial phenomenon that is characterized by the contact angle formed between a liquid drop and a solid surface.

B. Calculation of contact angle and surface energy

In addition to temperature and oxygen pressure, the surface interfacial energy between the film and substrate also plays a critical role in film growth. As water–metal oxide interactions with low electronegativity are primarily electrostatic, surface properties such as roughness, wettability, and surface energy are expected to be thickness-dependent. To further investigate this relationship, we measured the water contact angles (WCAs) of different liquids (water, glycerol, ethylene glycol, etc.) using the Shape Analyzer DSA 25-KRUSS GmbH. The contact angle was determined by the tangent to the solid–liquid–vapor triple point, where the drop shape was evaluated using Young's equation,

$$\cos(\theta) = \frac{\gamma_s - \gamma_{sl}}{\gamma_l}, \tag{2}$$

where θ is the contact angle, and γ_s, γ_{sl}, and γ_l are the surface energies of the substrate, the substrate–liquid interface, and the liquid, respectively (see Fig. 1).

By observing the contact angle between a solid surface and a liquid drop on the surface, it is possible to calculate the surface tension and wettability of a given solid material. A substrate is considered hydrophilic if the contact angle is less than 90°, indicating a high affinity for water molecules. Hydrophilic materials have active polar functional groups that enable them to adsorb water molecules. On the other hand, hydrophobic materials behave in the opposite way when interacting with water compared to hydrophilic materials, and parameters such as surface topography and energy determine the wetting behavior of the surface. The Owens–Wendt method (also known as the Kaelble–Owens–Wendt method)[19,20] is one of the few methods available for calculating surface energy components, namely, the dispersion and polar components. These components result from the Coulomb and van der Waals interactions between permanent and induced dipoles, and from temporary fluctuations caused by the charge distribution in the atom or molecules on the surface. The method is based on Berthelot's hypothesis, which assumes that the work of adhesion between a solid and a liquid is equal to the geometric mean of the cohesion work of a solid and the work of cohesion of the measuring liquid.

The geometric mean of the polar component (γ^p) and dispersive component (γ^d) of the surface tensions of liquids and of the surface energy of solids is given by the following equation:

$$\gamma_{sl} = \gamma_s + \gamma_l - 2\sqrt{(\gamma_s^d \gamma_l^d)} - 2\sqrt{(\gamma_s^p \gamma_l^p)}. \tag{3}$$

Using Eqs. (2) and (3), a linear equation such as $y = ax + b$ is attained,

$$\frac{(\gamma_l(1+\cos(\theta)))}{(2\sqrt{(\gamma_l^d)})} = \sqrt{(\gamma_l^d)}\frac{\sqrt{(\gamma_l^p)}}{(\sqrt{\gamma_l^d})} + \sqrt{\gamma_s^d}, \tag{4}$$

where $y = \frac{(\gamma_l(1+\cos(\theta)))}{(2\sqrt{(\gamma_l^d)})}$ and $x = \frac{\sqrt{\gamma_l^p}}{\sqrt{\gamma_l^d}}$ contain the known values such as the contact angle, the dispersive γ_l^d, and the polar γ_l^p parts of the liquid surface tension for each liquid. The linear regression of Eq. (4) primes straight to the components of the solid surface energy $\gamma_s^p = a^2$ and $\gamma_s^d = b^2$ with the total surface energy given by

$$\gamma_s = \gamma_s^p + \gamma_s^d, \tag{5}$$

where γ_s is the total surface energy, and γ_s^p and γ_s^d are the polar and dispersive components, respectively.

C. Derivation and culture of human bone marrow mesenchymal stem cells (hBMMSCs)

Bone marrow was collected from the iliac crests of adult donors undergoing arthroplasty who had signed an agreement form approved by the local ethical committee. The marrow was aspirated and the cells were fractionated using a Hypaque-Ficoll density gradient. Mononuclear cells were then isolated, seeded at a density of 5×10^4 cells/cm^2, and cultured in α-MEM supplemented with 10% fetal calf serum (Invitrogen^{TM}, Cergy-Pontoise, France), an L-glutamine of 2 mM, an FGF-2 of 1 ng/ml (Sigma-Aldrich, Saint Quentin Fallavier, France), and antibiotics. Once the cells reached ~80% confluency, they were harvested by trypsinization (using 0.25% trypsin/1 mM EDTA, Invitrogen) and seeded at 2×10^3 cells/cm^2. After five passages, the cells were checked for the absence of hematopoietic markers using reverse transcription-polymerase chain reaction (RT-PCR), and these hBMMSCs were then used for experiments. The media were changed three times per week, and the cells were maintained in a 5% CO_2 atmosphere at 37 °C.

D. Cell adhesion and proliferation

To assess cell adhesion and proliferation, hBMMSCs were seeded onto various substrates, including thin films of VO_x, uncoated glass, and plastic wells as a control, at a density of 10^4 cells/cm^2 in 24-well plates with α-MEM medium. After a 2-h incubation period, non-adherent cells were removed by washing them with phosphate-buffered saline (PBS). Adherent hBMMSCs were subsequently harvested by trypsinization (0.25% trypsin/1 mM EDTA, Invitrogen) and counted using the Countess^{TM} II Automated Cell Counter (Thermo Fisher Scientific) and trypan blue staining. The same procedure was repeated at different time points (24 h and 10 days) to monitor cell proliferation.

E. Differentiation assays

Seven days after seeding, differentiation (adipogenic, chondrogenic, and osteogenic) media were added, and cells were cultured for an additional 2 weeks, with media changes twice a week. Afterward, they were prepared for staining and gene expression. Composition media: Osteogenic medium (MEM α supplemented with 0.1% antibiotics, 10% FBS, a dexamethasone of 100 nM, an ascorbic acid-2 phosphate of 50 μg/ml , a β-glyceraldehyde of 10 μM), adipogenic medium: (MEM α with 0.1% antibiotics, 10% FBS, a dexamethasone of 100 nM, an Isobutylmethylxanthanine of 0.5 mM), or chondrogenic medium: [Dulbeccoś Modified Eagleś Medium-high glucose with glutamine and sodium pyruvate (DMEM, Dutcher), 0.1% antibiotics, a dexamethasone of 100 nM, an ascorbic acid-2 phosphate of 50 μg/ml, a proline of 40 μg/ml, transforming growth factor β-3 (TGF beta 3), and Insulin Transferrin Selenium media supplement $x(ITS + 1)$]. (All materials are from Sigma-Aldrich unless mentioned.)

F. Histological staining

To investigate the differentiation activity of cells on oxide thin films, oil red, alizarin red, and alcian blue staining were done. After 2 weeks of differentiation assay, the cells were fixed with 4% paraformaldehyde (PFA), and after being washed with phosphate-buffered saline (PBS), cells were kept at 4 °C in PBS. The staining tests consist of washing with distilled water (H2Od) and incubation with alcian blue, alizarin red, or oil red solutions for 30 min. After alizarin red and oil red staining, samples were washed four times with H2Od and fixed on microscopic histological glass slides. After alcian blue staining, samples were washed with H2Od, and cell layers were analyzed in 1% sodium dodecyl sulfate (SDS). Aliquots of the lysates were transferred to a 48-well plate, and absorbance at 616 nm was determined for triplicate samples (Multiskan GO spectrophotometer, Thermo Scientific^{TM}).

G. Real-time reverse polymerase chain reaction

Aside from histological staining, RNA was extracted by using a Qiagen kit (RNeasy® mini kit 250), according to the manufacturer's protocol. Total RNA (1 μg) was treated with DNAse before reverse transcription into cDNA using the MMLV enzyme (Invitrogen by Thermo Fisher Scientific) and oligo T primers. Specific transcripts were then amplified by real-time PCR on the StepOnePlus apparatus (Thermo Fisher Scientific) targeting (RUNX2), chondrogenic (COL2A1), and adipogenic (CEBP/a) genes. Reactions were done using Power SYBR Green mix (Thermo Fisher Scientific) for 40 cycles (30 s at 95 °C/1 min at 60 °C). GAPDH, RPL13, and B2MG

TABLE I. Primer sequences used for RT-PCR analysis.

Gene	Primer
OST (osterix)	F: GGCTCAGCTCTCTCCATCTC
	R: GGGGACTGGAGCCATAGTG
CBPa (CCAAT enhancer-binding protein alpha)	F: ACTGGGACCCTCAGCCTTG
	R: TGGACTGATCGTGCTTCGTG
ACAN (aggrecan)	F: GTGCCTATCAGGACAAGGTCT
	R: GATGCCTTTCACCACGACTTC
GAPDH (glyceraldehyde-3-phosphate dehydrogenase)	F: ATGGGGAAGGTGAAGGTCG
	R: TAAAAGCAGCCCTGGTGACC
RPL13 (ribosomal protein L13)	F: GTTCGGTACCACACGAAGGT
	R: CTGGGGAAGAGGATGAGTTTG
B2MG (beta-2-microglobulin)	F: GAGGCTATCCAGCGTACTCCA
	R: CGGCAGGCATACTCATCTTTT

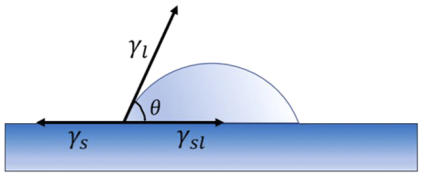

FIG. 1. Schematic diagram illustrating the components of the contact angle.

housekeeping genes were used to normalize mRNA expression levels calculated by the 2 – ΔΔ Ct method. The sequences of the primers used are given in Table I.

Standard α-MEM medium was used for cell culture, and differentiation media were introduced after one week of culture. The media were refreshed twice a week. Total RNA was extracted from cells cultured in osteogenic and chondrogenic media for 16 days using a RNeasy Mini kit (Qiagen), according to the manufacturer's instructions. Next, an extracted RNA of 500 ng was reverse transcribed into cDNA using an Invitrogen kit after the DNAse I treatment. The $2^{-\Delta\Delta Ct}$ method was used to calculate mRNA expression levels, which were normalized using the GAPDH, RPL13, and B2MG housekeeping genes.

III. RESULTS AND DISCUSSION

A. Film characterization

Before conducting the *in vitro* experiments, various techniques were utilized to characterize the vanadium dioxide films and gather information about their properties, including thickness, roughness, and wettability. Surface roughness was evaluated using the AFM technique, and the surface profiles of the control sample (uncoated glass slide) and VO_x film deposited at 400 °C were compared in Figs. 2(a) and 2(b). The roughness was found to slightly increase with film thickness, where the roughness of a 6 nm film was ~0.20 nm and that of a 26 nm film was 0.79 nm. The roughness of the uncoated glass substrate was ~0.1 nm, while the VO_x samples had a roughness in a range of 0.2–0.8 nm, indicating a smooth surface of the films and good quality of the PLD-grown VO_x thin films.

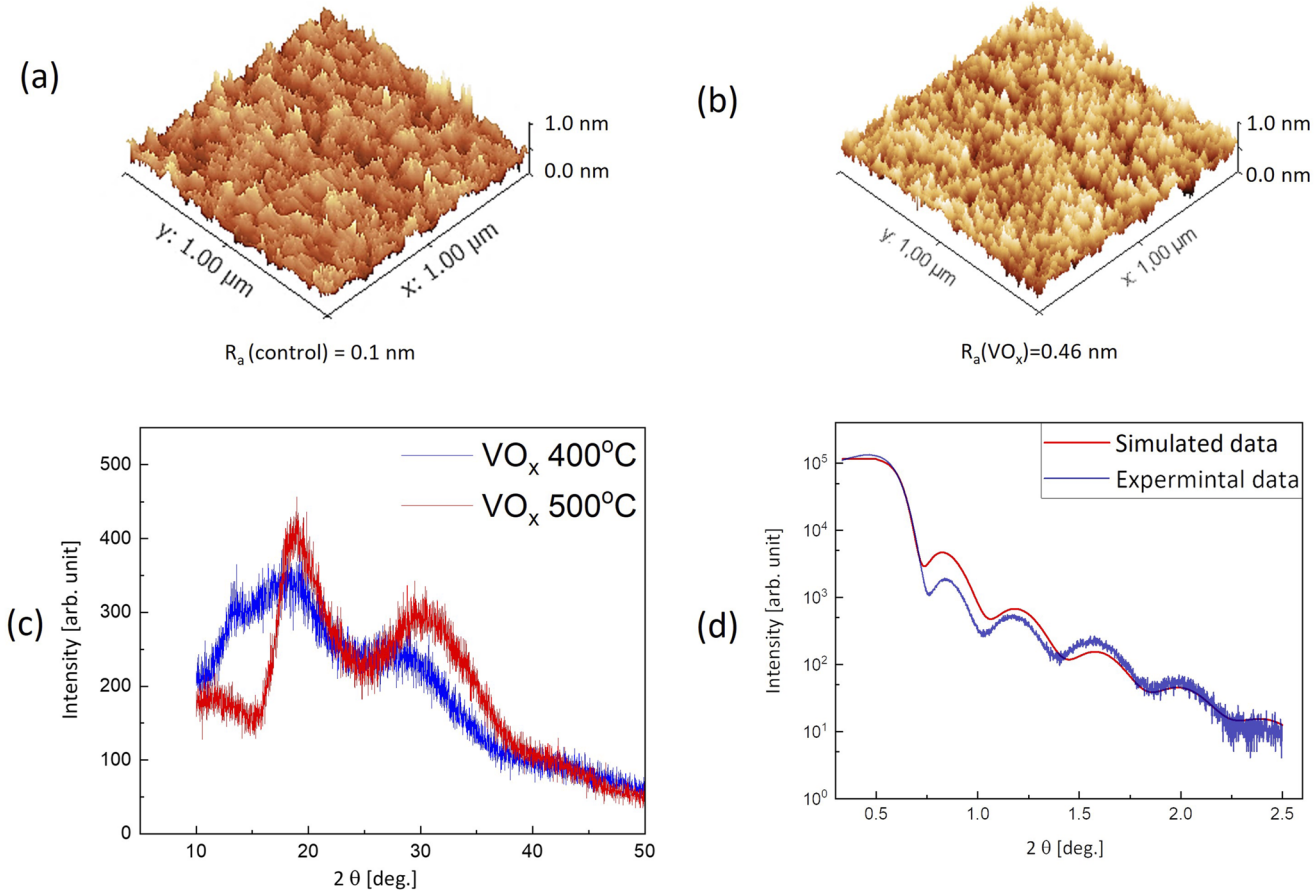

FIG. 2. AFM images showing the surface profiles of the glass substrate (control) (a) and VO_x thin films (b). The corresponding average roughness (R_a) is indicated below each figure. Typical VO_x thin films were analyzed for their XRD patterns (c) and XRR curves (d).

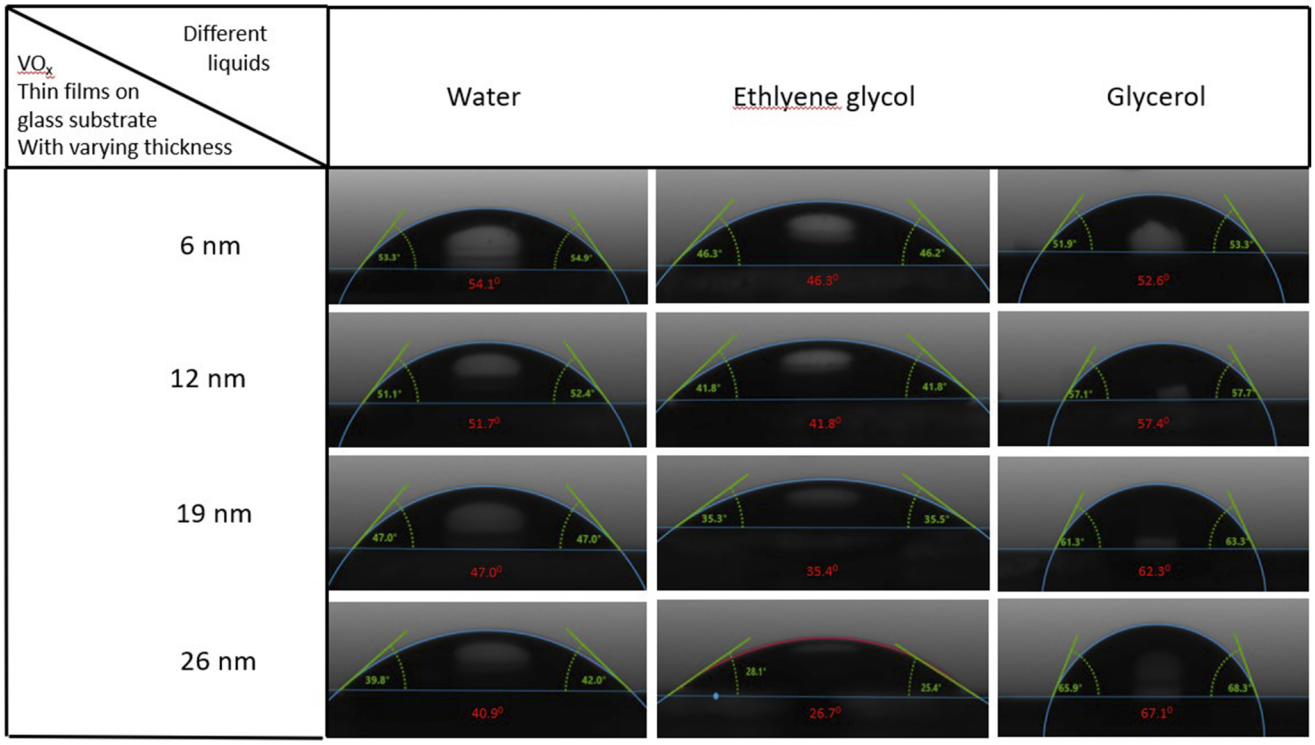

FIG. 3. Contact angle images of vanadium oxide thin films with different testing liquids (water, ethylene glycol, and glycerol) are shown. The thickness of the films is also indicated against each figure.

Although vanadium oxides can exhibit different stoichiometries depending on temperature and other growth conditions, XRD measurements revealed that the deposited thin films had an amorphous structure [Fig. 2(c)]. This is evident from the two broad peaks of low intensity, indicating the absence of long-range ordering in the structure. Hence, x-ray diffraction analysis does not provide information about the stoichiometry or structure of the vanadium oxide, and the composition of the vanadium oxide thin films will be referred to as VO_x in the following. The thickness of the films was extracted from Fig. 2(d) using the XRR technique, ranging from 6 to 26 nm, resulting in a deposition rate of ~0.012 nm/laser pulse.

When droplets of distilled water, ethylene glycol, and glycerol were placed on VO_x thin films of varying thickness, the contact angle for all droplets was less than 90° (see Fig. 3), indicating that the films were hydrophilic in nature. This hydrophilicity can be attributed to the presence of surface hydroxyl groups on the metal oxide thin films, which can easily form hydrogen bonds with water molecules.[21]

Figure 4 shows the evolution of the contact angle with the thickness of VO_x thin films. The contact angle values of distilled water droplets on VO_x thin films with thicknesses of 6, 12, 19, and 26 nm were 54.1°, 51.7°, 47.0°, and 40.9°, respectively, and with ethylene glycol were 46.3°, 41.8°, 35.4°, and 26.7°, respectively. It was observed that the contact angle decreased with increasing thickness. Tungsten-doped vanadium dioxide (VO_2) thin films deposited on fused quartz were found to be extremely hydrophilic, yielding similar results. In addition, iron dopants in VO_2 thin films resulted in smaller water contact angles, indicating superior hydrophilic properties.[22] This phenomenon can be explained by the Wenzel equations mentioned earlier, which indicates that an increase in roughness with thickness results in increased hydrophilicity of these surfaces as observed.

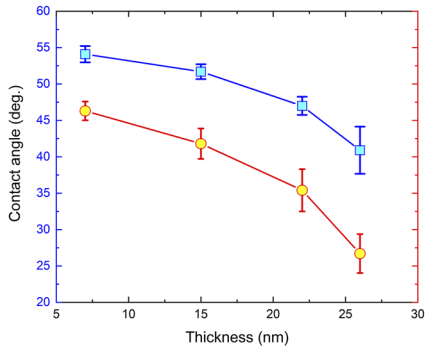

FIG. 4. Variation of the magnitude of the contact angle with respect to the thickness of VO_x thin films. The contact angle with water and ethylene glycol is represented by the symbols ■ and ○, respectively.

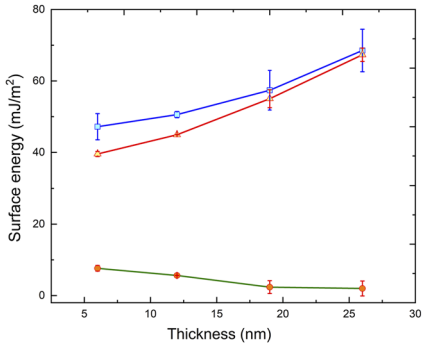

FIG. 5. Evolution of total surface energy (■) and its polar (●) and dispersive (▲) components with varying thickness of the VO_x thin films.

B. Surface energy properties of VO_x thin films

We used Eqs. (4) and (5) to calculate the total surface energy of VO_x thin films, which varied from 47 to 69 mJ/m^2. To obtain the surface free energy, we employed the dispersive (γ_l^d) fractions reported previously, which were 21.8, 34, and 29 for water, ethylene glycol, and glycerol, respectively, as well as the polar (γ_l^p) fractions, which were 51.0, 30.4, and 19.3 mJ/m^2 for the same liquids.

For the 6 nm VO_x thin film, the polar, dispersive, and total surface energies were 7.63, 39.56, and 47.19 mJ/m^2, respectively. For the 26 nm thin film, the polar, dispersive, and total surface energies were 1.20, 67.32, and 68.52 mJ/m^2, respectively, as shown in Fig. 5. The polar component of the surface energy decreased with increasing thickness due to weaker Coulomb interactions between permanent and induced dipoles. Figure 5 also revealed that the dispersive component contributed significantly to the surface energy, which was related to van der Waals interactions resulting from charge motion at the thin film surface.

The reason for this phenomenon could be attributed to the different oxidation states of vanadium, which react differently with liquids depending on their polarity. In addition, the variation in particle size distributions during the pulsed laser deposition (PLD) growth of VO_x thin films could lead to higher packing efficiency of powder beds, resulting in a lower wetting effect, a decreased contact

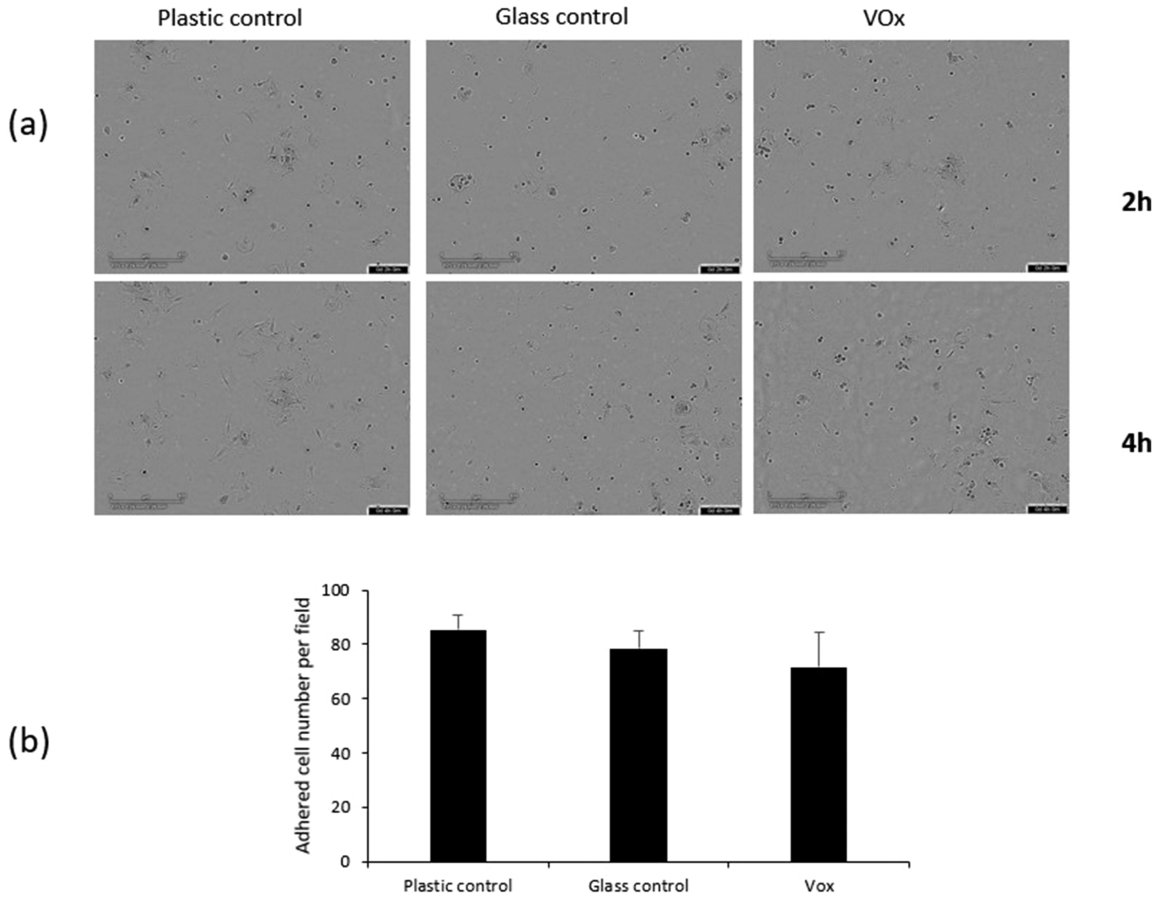

FIG. 6. Cell density of hBMMSCs cultured on glass and plastic control and VO_x thin films after 2 h of culture. (a) Phase contrast images of hBMMSCs on glass control and VO_x surfaces were recorded after 10 days of culture (scale bar = 400 μ m). (b) shows the corresponding cell density of glass and plastic control vs VO_x surfaces, respectively.

angle (better wetting), and increased surface energy.[23] To confirm the oxidation state of vanadium, we are currently conducting x-ray photoelectron spectroscopy (XPS), and the results will be published in a separate publication.

C. Adhesion and proliferation of hBMMSCs on VO_x thin films

We assessed the initial adhesion of cells onto substrates at 2 and 4 h [see Fig. 6(a)] and captured several microphotographs. Cell counting was performed and indicated that there were only slight differences in cell adhesion between vanadium oxide films and bare glass or plastic substrates. However, the adhesion of hBMMSCs to vanadium appeared to be somewhat lower, although the difference was not significant. In addition, we captured microscopy images after 10 days to monitor cell proliferation and growth (given in the supplementary data video 10 days). The obtained images revealed that cells cultured on plastic and glass substrates had reached confluence, while those cultured on VO_x did not completely cover the surface, likely due to the lower initial adhesion observed. Therefore, our results suggest that VO_x interferes with hBMMSCs adhesion but does not impact cell growth.

Although there are no published works using vanadium oxides for human mesenchymal stem cell culture, a few articles exist on vanadium compounds used with other types of cells. For example, Srivastava *et al.* investigated the ability of V(IV) oxides to control the osteoblastic differentiation of C3H10t1/2 mouse cells.[24] Their results show that V (IV) oxide causes increased phosphorylation of the proteins ERK 12, IB, and NFBp65. Inhibition of osteoblast differentiation by ERK and NFB pathway inhibitors was abolished in the presence of V (IV) oxide, as demonstrated by RT-PCR, alizarin red staining, and immunoblot analysis. These results suggest that V (IV) oxide can stimulate osteoblast differentiation via the ERK and NFB signaling pathways, suggesting its potential as an agent for bone formation.[24] Vanadium oxides have also been used in the form of nanotubes and found to be cytotoxic to human colon carcinoma cells by Rhoads *et al.* who showed that these cells lost viability after a few hours.[25]

D. Influence of VO_x coating on chondrogenic, osteogenic, and adipogenic differentiation of hBMMSCs

To assess the influence of VOx oxide films on the differentiation potential of hBMMSCs, cells were seeded on VO_x thin films, uncoated glass, or regular plastic wells. After adhesion for 48 h, they were cultured for 2 weeks under a regular medium (control) before fixing and preparing the cell layers for cytological staining, namely Alcian blue (proteoglycans accumulation), Alizarin red (calcium-rich sites of mineralization), and Oil red. Figure 7 illustrates that culturing hBMMSCs on VO_x substrate affects their differentiation. They exhibit more proteoglycan accumulation (Alcian blue staining) and fewer calcium sites of mineralization (Alizarin red), while calcium sites of mineralization (Alizarin red) and the number of lipidic vesicles remain unchanged (Oil red) (lipidic vesicles staining). Parallel cultures were also conducted under specific media that direct the cells toward chondrogenic, osteogenic, or adipogenic differentiation. When seeded on plastic or glass wells, hBMMSCs show good trilineage differentiation, with clear staining with Alcian blue, Alizarin red, and Oil red in comparison to respective controls. However, culture on VO_x thin films alters the behavior of the cells by altering osteogenic differentiation while enhancing adipogenic differentiation.

To confirm the observations made by cytological staining, gene expression analysis was done on parallel cultures. HBMMSCs were cultured on VO_x thin films, uncoated glass, and plastic wells for 2 weeks. In order to observe the net effect of the oxides vs control on differentiation, we culture the cells only with regular media, without those that enhance their differentiation.

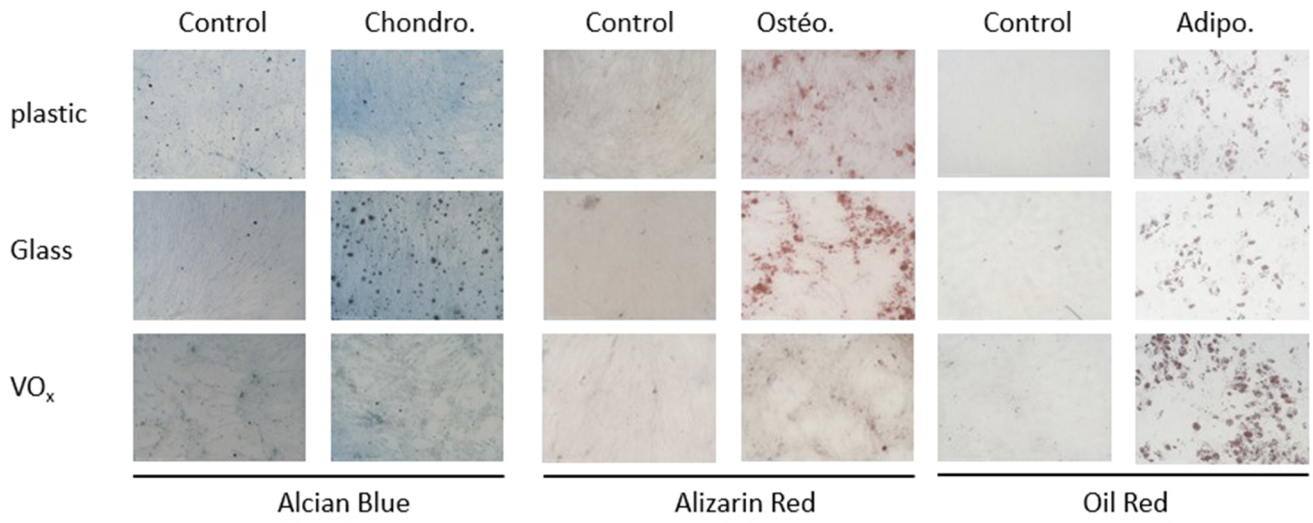

FIG. 7. Cytological staining with alcian blue, alizarin red, or oil red for hBMMSCs differentiation potential. Microphotographs were taken using a bright-field microscope at a magnification of 10×.

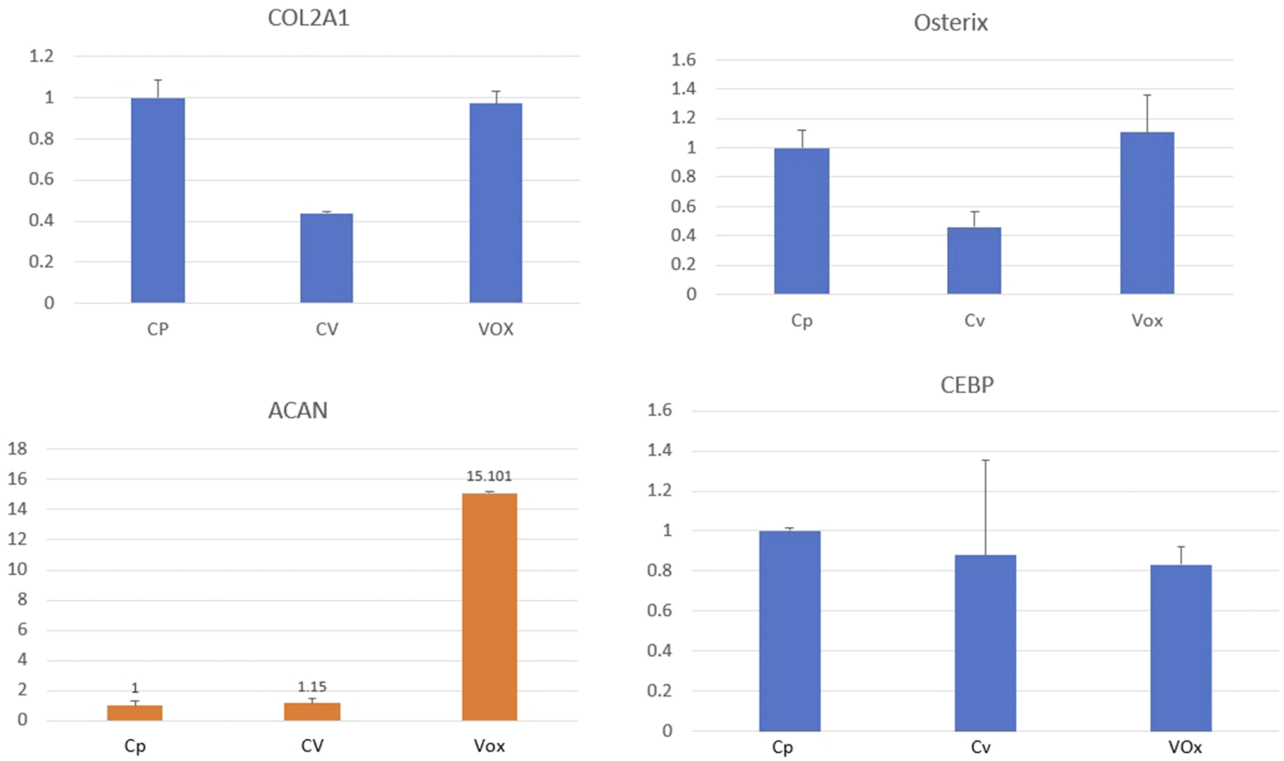

FIG. 8. Chondrogenic (COL2A1 and ACAN), Osteogenic (OSTERIX), and adipogenic (CEBP) differentiation of hBMMSCs on plastic, glass, and VO_x thin film substrates after 14 days of culture. A statistical evaluation was performed by comparing the samples with the glass and plastic substrates.

RNA was extracted, and real-time RT-PCR analysis was performed for specific gene expression. Figure 8 shows the normalized expression of COL2A1 and ACAN (for chondrogenic lineage), Osterix (for osteogenic), and C/EBPalpha (for adipogenic lineage) with GAPDH, RPL13, and B2MG as housekeeping genes. However, while Osterix and C/EBPa expressions are unaffected, ACAN expression is greatly enhanced when the cells are in contact with VO_x (as shown in Fig. 8). These observations are consistent with cytological staining that showed more proteoglycan production under culture on VO_x while no mineralization or lipidic vesicles were seen.

IV. CONCLUSION

To summarize, we employed the pulsed laser deposition technique to create thin films of vanadium oxide (VO_x), which we then used as substrates for the development of human bone marrow mesenchymal stem cells (hBMMSCs). The VO_x coatings had flat surfaces that were hydrophilic in nature. According to the findings of our comprehensive investigation, the VO_x films had a marginally inhibitive effect on the adhesion and proliferation of hBMMSCs, although this effect was not statistically significant. Furthermore, we found that VO_x coatings promote chondrogenesis while having some influence on osteogenic or adipogenic differentiation. These findings are corroborated by cytological staining as well as real-time RT-PCR gene expression analyses. Our findings emphasize the necessity of understanding the mechanisms and reactions behind vanadium oxide's impacts on cell behavior, notably the relevance of surface chemistry and morphology in the materials' interaction with cells. When exploiting such surfaces to construct cell culture substrates for screening tests and perhaps orthopedic prostheses, this is extremely crucial.

SUPPLEMENTARY MATERIAL

The supplementary material consists of media files pertaining to Section C describing the adhesion and proliferation of hBMMSCs on VO_x thin films corresponding to cell culture on glass (Extension 1), plastic (Extension 2) substrates, and VO_x (Extension 3) thin films for 10 days.

ACKNOWLEDGMENTS

We thank F. Ferreira, X. Larose, and J. Lecourt for their technical support. M.K., A.Y., M.H., and E.L. received their Ph.D. scholarship from the UNICAEN and Normandie University. Partial support from LAFICS was also acknowledged. This work was done under the Program Emergence "InCox" and "CiBox" supported by the Region Normandie.

AUTHOR DECLARATIONS

Conflict of Interest

The authors have no conflicts to disclose.

Author Contributions

Maria Khokhlova and Abhishek Yadav contributed equally to this work.

Maria Khokhlova: Investigation (equal); Writing – original draft (equal); Writing – review & editing (equal). **Abhishek Yadav**: Investigation (equal); Writing – original draft (equal); Writing – review & editing (equal). **M. Hammad**: Investigation (equal). **Eva Lhuissier**: Investigation (equal). **R. Retoux**: Investigation (equal). **D. Goux**: Investigation (equal). **Arnaud Fouchet**: Investigation (equal). **Adrian David**: Investigation (equal). **Ulrike Luders**: Investigation (equal). **Karim Boumediene**: Investigation (equal); Writing – original draft (equal); Writing – review & editing (equal). **W. Prellier**: Funding acquisition (equal); Methodology (equal); Supervision (equal); Writing – original draft (equal); Writing – review & editing (equal).

DATA AVAILABILITY

The data that support the findings of this study are available from the corresponding author upon reasonable request.

REFERENCES

[1]M. Lorenz, M. S. Ramachandra Rao, T. Venkatesan, E. Fortunato, P. Barquinha, R. Branquinho, D. Salgueiro, R. Martins, E. Carlos, A. Liu *et al.*, "The 2016 oxide electronic materials and oxide interfaces roadmap," J. Phys. D: Appl. Phys. **49**, 433001 (2016).

[2]P. Liu, S.-H. Lee, C. E. Tracy, J. A. Turner, J. R. Pitts, and S. K. Deb, "Electrochromic and chemochromic performance of mesoporous thin-film vanadium oxide," Solid State Ionics **165**, 223–228 (2003).

[3]R. Ramesh and D. G. Schlom, "Whither oxide electronics?," MRS Bull. **33**, 1006–1014 (2008).

[4]M. Khokhlova, M. Hammad, E. Lhuissier, R. Retoux, D. Goux, A. Fouchet, A. David, U. Lüders, K. Boumediene, and W. Prellier, "Differentiation of mesenchymal stem cells using metal oxide thin films," J. Phys. D: Appl. Phys. **54**, 235402 (2021).

[5]C. Boudot, M. Kühn, M. Kühn-Kauffeldt, and J. Schein, "Vacuum arc plasma deposition of thin titanium dioxide films on silicone elastomer as a functional coating for medical applications," Mater. Sci. Eng.: C **74**, 508–514 (2017).

[6]B. C. Costa, C. K. Tokuhara, L. A. Rocha, R. C. Oliveira, P. N. Lisboa-Filho, and J. C. Pessoa, "Vanadium ionic species from degradation of Ti-6Al-4V metallic implants: In vitro cytotoxicity and speciation evaluation," Mater. Sci. Eng.: C **96**, 730–739 (2019).

[7]M. M. Dykas, S. K. Desai, A. Patra, M. R. Motapothula, K. Poddar, L. J. Kenney, and T. Venkatesan, "Identification of biofilm inhibitors by screening combinatorial libraries of metal oxide thin films," ACS Appl. Mater. Interfaces **10**, 12510–12517 (2018).

[8]D. A. Barrio, M. D. Braziunas, S. B. Etcheverry, and A. M. Cortizo, "Maltol complexes of vanadium (IV) and (V) regulate in vitro alkaline phosphatase activity and osteoblast-like cell growth," J. Trace Elem. Med. Biol. **11**, 110–115 (1997).

[9]B. Moretti, V. Pesce, G. Maccagnano, G. Vicenti, P. Lovreglio, L. Soleo, and P. Apostoli, "Peripheral neuropathy after hip replacement failure: Is vanadium the culprit?," Lancet **379**, 1676 (2012).

[10]C. Tosat-Bitrián and V. Palomo, "CdSe quantum dots evaluation in primary cellular models or tissues derived from patients," Nanomed.: Nanotechnol., Biol. Med. **30**, 102299 (2020).

[11]Q. Zhou, Z. Zhao, Z. Zhou, G. Zhang, R. C. Chiechi, and P. van Rijn, "Directing mesenchymal stem cells with gold nanowire arrays," Adv. Mater. Interfaces **5**, 1800334 (2018).

[12]M. U. A. Khan, S. I. A. Razak, A. Hassan, S. Qureshi, G. M. Stojanović, and Ihsan-Ul-Haq, "Multifunctional arabinoxylan-*functionalized*-graphene oxide based composite hydrogel for skin tissue engineering," Front. Bioeng. Biotechnol. **10**, 865059 (2022).

[13]S. Nazir, M. U. A. Khan, W. S. Al-Arjan, S. I. Abd Razak, A. Javed, and M. R. A. Kadir, "Nanocomposite hydrogels for melanoma skin cancer care and treatment: *In-vitro* drug delivery, drug release kinetics and anti-cancer activities," Arabian J. Chem. **14**, 103120 (2021).

[14]J. Dai, X. Wang, S. He, Y. Huang, and X. Yi, "Low temperature fabrication of VO_x thin films for uncooled IR detectors by direct current reactive magnetron sputtering method," Infrared Phys. Technol. **51**, 287–291 (2008).

[15]D. Barreca, L. E. Depero, E. Franzato, G. A. Rizzi, L. Sangaletti, E. Tondello, and U. Vettori, "Vanadyl precursors used to modify the properties of vanadium oxide thin films obtained by chemical vapor deposition," J. Electrochem. Soc. **146**, 551 (1999).

[16]R. Dietsch, T. Holz, H. Mai, M. Panzner, and S. Völlmar, "Pulsed laser deposition (PLD)—An advanced state for technical applications," Opt. Quantum Electron. **27**, 1385–1396 (1995).

[17]I. Horcas, R. Fernández, J. M. Gómez-Rodríguez, J. Colchero, J. Gómez-Herrero, and A. M. Baro, "WSXM: A software for scanning probe microscopy and a tool for nanotechnology," Rev. Sci. Instrum. **78**, 013705 (2007).

[18]R. N. Wenzel, "Resistance of solid surfaces to wetting by water," Ind. Eng. Chem. **28**, 988–994 (1936).

[19]D. K. Owens and R. C. Wendt, "Estimation of the surface free energy of polymers," J. Appl. Polym. Sci. **13**, 1741–1747 (1969).

[20]D. H. Kaelble, "Dispersion-polar surface tension properties of organic solids," J. Adhes. **2**, 66–81 (1970).

[21]M. Miyauchi, A. Nakajima, T. Watanabe, and K. Hashimoto, "Photocatalysis and photoinduced hydrophilicity of various metal oxide thin films," Chem. Mater. **14**, 2812–2816 (2002).

[22]Z. Liang, L. Zhao, W. Meng, C. Zhong, S. Wei, B. Dong, Z. Xu, L. Wan, and S. Wang, "Tungsten-doped vanadium dioxide thin films as smart windows with self-cleaning and energy-saving functions," J. Alloys Compd. **694**, 124–131 (2017).

[23]E. Müller, W. Vogelsberger, and H.-G. Fritsche, "The dependence of the surface energy of regular clusters and small crystallites on the particle size," Cryst. Res. Technol. **23**, 1153–1159 (1988).

[24]S. Srivastava, N. Kumar, and P. Roy, "Role of ERK/NFκB in vanadium (IVoxide mediated osteoblast differentiation in C3H10t1/2 cells," Biochimie **101**, 132–144 (2014).

[25]L. S. Rhoads, W. T. Silkworth, M. L. Roppolo, and M. S. Whittingham, "Cytotoxicity of nanostructured vanadium oxide on human cells in vitro," Toxicol. In Vitro **24**, 292–296 (2010).